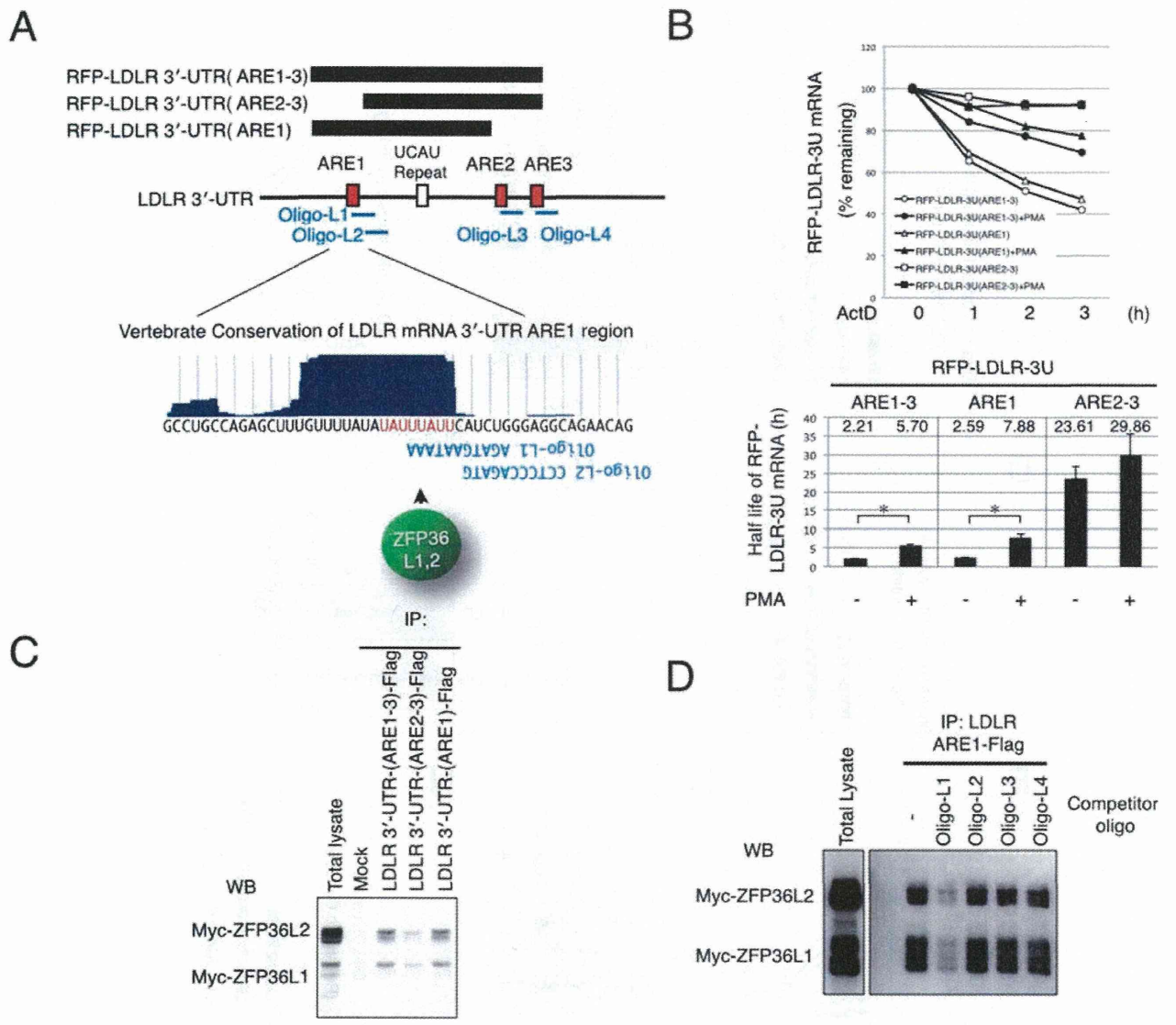

Figure 2. Domain analysis of the 3′-UTR of LDLR mRNA. (**A**) Schematic representation of the 3′-UTR of LDLR mRNA. Black bars indicate the regions used for ActD chase and IP experiments. AREs 1–3 are indicated by red boxes and the UCAU repeat is indicated by the white box. Designed oligonucleotides are indicated by blue lines. Conservation around the LDLR ARE1 region is shown in the blue graph, created using Vertebrate Multiz Alignment & PhastCons Conservation (28 species), as extracted from the UCSC Human Genome Browser (http://genome.ucsc.edu/). The consensus ZFP36L1- and ZFP36L2-binding sequence is colored in red. Sequences of the designed oligonucleotides, L1 and L2, are indicated. (**B**) RFP-tagged LDLR 3′-UTR constructs were expressed in 293T cells, and cells were then subjected to ActD chase experiments. Twenty-four hours after transfection, 293T cells were treated with ActD and PMA as indicated (PMA treatment commenced 10 min after ActD treatment). qPCR was performed using RFP and Luc2-specific primers. Results were normalized to the levels of Luc2 mRNA. The data are representative of at least three independent experiments. mRNA half-lives were calculated by fitting an exponential decay curve to all time points. Figures in the graph indicate the mean value of the mRNA decay half-lives. Error bars show standard deviation of the mean. *P*-values were calculated using Student's *t*-test. $*P < 0.002$; $n = 3$ for each group. (**C**) 293T cells were transfected with Myc-tagged ZFP36L1 and ZFP36L2. Cells were then lysed with lysis buffer and the cleared lysates were subjected to IP with the indicated LDLR 3′-UTR bait RNAs. Immunoprecipitated proteins were subjected to western blot analysis with the anti-Myc antibody. (**D**) 293T cells were transfected with Myc-tagged ZFP36L1 and ZFP36L2. Cells were then lysed with lysis buffer and the cleared lysates were subjected to IP with the indicated LDLR 3′-UTR bait RNAs and the indicated oligos. Immunoprecipitated proteins were subjected to western blot analysis with the anti-Myc antibody. These data are representative of at least three independent experiments.

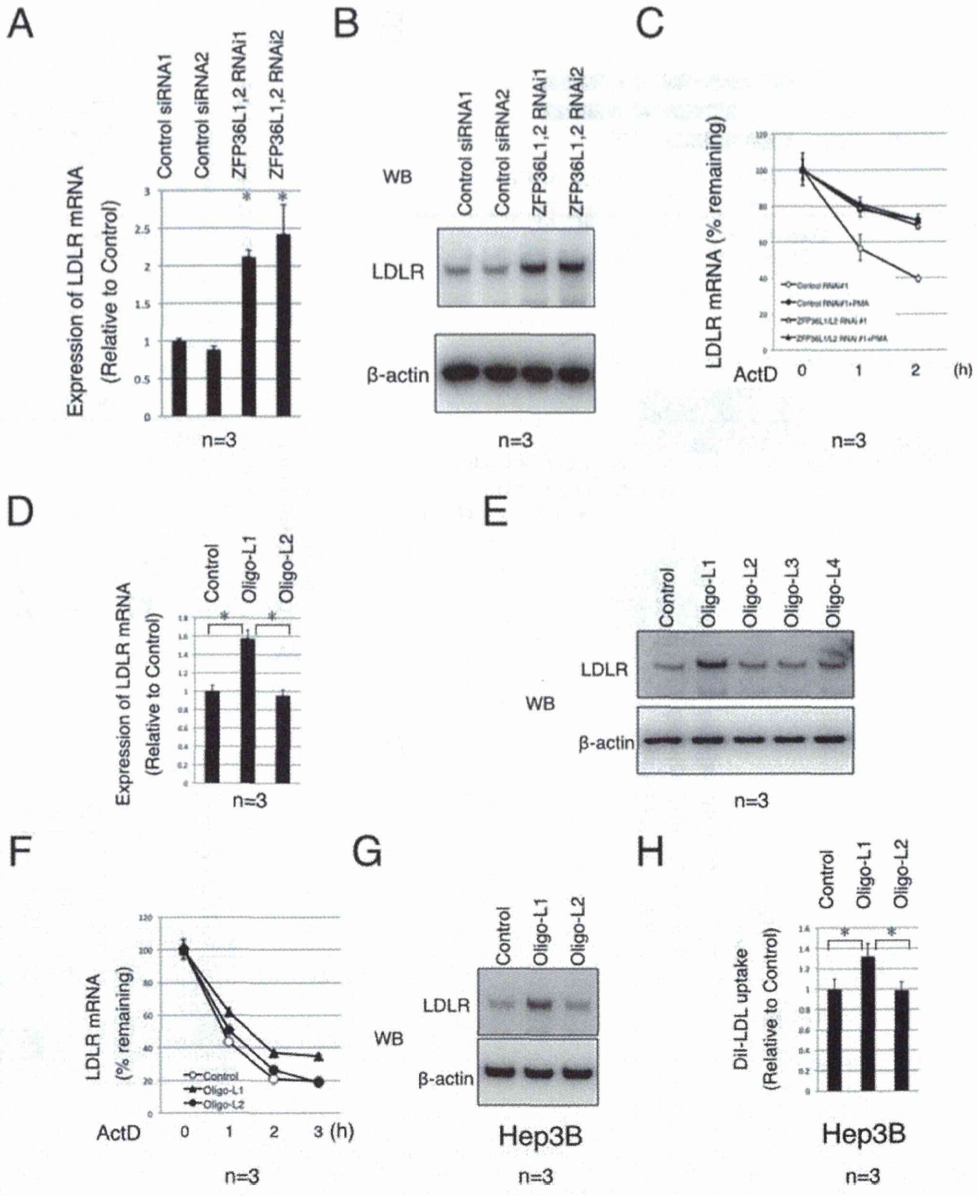

Figure 3. LDLR mRNA is destabilized by ZFP36L1 and ZFP36L2. (**A**) HeLa cells were transfected with ZFP36L1 and ZFP36L2 siRNAs. Forty-eight hours after transfection, cells were harvested, total RNA was extracted and quantitative RT-PCR (qPCR) was performed using primers specific to LDLR mRNA and β-actin mRNA. Results were normalized to β-actin mRNA levels. Error bars show standard deviation of the mean. *P*-values against control were calculated using Student's *t*-test.*$P < 0.002$; $n = 3$ for each group. (**B**) Forty-eight hours after transfection, cells were harvested and the lysates were subjected to western blot analysis using the indicated antibodies. (**C**) Forty-eight hours after transfection, cells were treated with ActD and chased for the indicated time with or without PMA (PMA treatment commenced 10 min after ActD treatment). Total RNA was extracted and qPCR was performed using primers specific to LDLR mRNA and β-actin mRNA. Results were normalized to the levels of β-actin mRNA. Error bars show standard deviation of the mean. (**D**) HeLa cells were transfected with the indicated oligos. Twenty-four hours after transfection, cells were harvested and total RNA was extracted. Quantitative RT-PCR (qPCR) was performed using primers specific for LDLR and β-actin. Results were normalized to β-actin mRNA levels. Error bars show standard deviation of the mean. *P*-values against control were calculated using Student's *t*-test. *$P < 0.002$; $n = 3$ for each group. (**E**) HeLa cells were transfected with the indicated oligos. Twenty-four hours after transfection, cells were harvested and the lysates were subjected to western blot analysis using the indicated antibodies. (**F**) HeLa cells were transfected with the indicated oligos. Twenty-four hours after transfection, cells were treated with ActD and chased for the indicated times. Total RNA was extracted and qPCR was performed using primers specific to LDLR mRNA and β-actin mRNA. Results were normalized to the levels of β-actin mRNA. Error bars show standard deviation of the mean. (**G**) Hep3B cells were transfected with the indicated oligos. Twenty-four hours after transfection, cells were harvested and the lysates were subjected to western blot analysis using the indicated antibodies. (**H**) Hep3B cells were transfected with the indicated oligos. Twenty-four hours after transfection, cells were treated with DiI-LDL for 1 h. The cells were then lysed in RIPA buffer and the ratio of DiI-LDL fluorescence/protein concentration was measured. Error bars show standard deviation of the mean. *P*-values against control were calculated using Student's *t*-test. *$P < 0.002$; $n = 3$ for each group. The data are representative of at least three independent experiments. The number below the figure indicates the number of times we replicated the experiment. Data from one of the independent experiments are shown in Supplementary Figure S4A–H.

that this regulation is conserved among these cells (Supplementary Figure S3D).

To further confirm that the ZFP36L1 and ZFP36L2-mediated destabilization of LDLR mRNA is caused by direct interaction, we examined the effect of LNA-modified oligonucleotides (as used in the experiment presented in Figure 2D) on the levels of LDLR mRNA and LDLR protein. We transfected these oligonucleotides into HeLa cells and found that Oligo-L1 increased the levels of LDLR mRNA and protein (Figure 3D and E, Supplementary Figure S3E). In contrast, Oligo-L2, -L3 and -L4 had no effect on the levels of LDLR mRNA or protein (Figure 3D and E, Supplementary Figure S3E). In addition, as expected, Oligo-L1 had no effect on the levels of VEGFA or PLK3 mRNAs (Supplementary Figure S3F). We also examined the effect of Oligo-L1 on the stability of LDLR mRNA in HeLa and 293T cells using an ActD chase experiment and we found that Oligo-L1 stabilized LDLR mRNA in these cell lines (Figure 3F, Supplementary Figure S3G and H). We then used two further oligonucleotides, Oligo-L5 and Oligo-L6. Oligo-L5 is a point mutant of Oligo-L1 (T8G) and Oligo-L6 is a scrambled oligonucleotide of Oligo-L1. Neither of these oligonucleotides could inhibit the interaction between LDLR mRNA and ZFP36L1, nor could they increase the stability of LDLR mRNA or the levels of LDLR protein in cells (Supplementary Figure S3I and J)

We finally used human liver-derived Hep3B cells, because we anticipate that this approach could potentially increase the levels of LDLR protein in the liver, thereby lowering blood LDL cholesterol levels. We transfected Oligo-L1 and Oligo-L2 into Hep3B cells and again found that Oligo-L1 stabilized LDLR mRNA and increased the levels of LDLR protein (Figure 3G, Supplementary Figure S3K and L). We then examined the effect of these oligonucleotides on LDL incorporation in Hep3B cells using DiI-labeled LDL. As expected, we found that Oligo-L1 increased LDL incorporation into Hep3B cells (Figure 3H). These results indicate that, LNA-modified antisense oligonucleotides can increase the LDL-uptake activity of liver-derived cells.

ZFP36L1 is regulated by phosphorylation downstream of ERK

Next, we investigated the underlying mechanisms of PMA-ERK-mediated LDLR mRNA stabilization. Given that ERK is a critical kinase in PMA-mediated LDLR mRNA stabilization (4), we examined whether ZFP36L1 is phosphorylated downstream of ERK. We found that PMA treatment induced an electrophoretic mobility shift of ZFP36L1, which could be reversed when cells were treated with PMA and U0126, a specific inhibitor of the ERK pathway (Figure 4A). We also found that the mobility shift of Flag-ZFP36L1, which we immunopurified from Flag-ZFP36L1-overexpressing and PMA-treated 293T cells, could be reversed by treatment with bacterial alkaline phosphatase (Figure 4B). These results indicate that ZFP36L1 is phosphorylated downstream of ERK. We then analyzed the ERK-dependent phosphorylation sites using an iTRAQ-based quantitative MS approach. We immunopurified Flag-ZFP36L1 protein from mock-, PMA- or PMA + U0126-treated 293T cells and determined the ERK-dependent phosphorylation sites. We found that phosphorylation of the C-terminal serine-334 residue of ZFP36L1 and of the C-terminal serine-493 and -495 residues of ZFP36L2 was increased upon PMA treatment, but was reversed by U0126 treatment (Figure 4C, Supplementary Figure S5A). This result indicates that the phosphorylation of these residues is ERK -dependent. We also analyzed the phosphorylation of endogenous ZFP36L1, which we purified from 293T cell lysate using a Flag-tagged LDLR ARE1 region (Supplementary Table S1), and found that the C-terminal serine-334 residue of endogenous ZFP36L1 is also phosphorylated upon PMA treatment (Supplementary Figure S5B and C).

To understand the function of ZFP36L1 phosphorylation, we first examined whether PMA treatment decreases the RNA-binding ability of ZFP36L1 and ZFP36L2. We found that PMA treatment slightly increased the interaction between Myc-ZFP36L1 and LDLR mRNA, while that with Myc-ZFP36L2 was not affected by PMA treatment (Figure 4C). We found that the RNA-binding ability of endogenous ZFP36L1 was also slightly increased by PMA treatment (Supplementary Figure S5B). These results indicate that PMA treatment does not inhibit the RNA-binding ability of ZFP36L1 and ZFP36L2.

The CCR4-NOT deadenylase complex has recently been shown to interact with the C-terminus of ZFP36 (16,17); therefore, we next examined whether ZFP36L1 interacts with the CCR4-NOT deadenylase complex and whether this interaction is affected by PMA. We found that CNOT7, a critical enzymatic component of CCR4-NOT deadenylase, interacts with ZFP36L1 and interestingly, this interaction is inhibited by PMA treatment and reversed by U0126 treatment, indicating that this regulation is mediated by the ERK pathway (Figure 4E). To confirm that this effect was due to C-terminal phosphorylation, we constructed the ZFP36L1-ΔC mutant (in which C-terminal amino acid residues, including all conserved phosphorylation sites, were deleted) and the ZFP36L1-SASA mutant (in which serine-334 and -336 were mutated to alanine residues, mimicking constitutive de-phosphorylation) (Figure 4F). We then examined the interaction between CNOT7 and these ZFP36L1 mutants and found that the ZFP36L1-SASA mutant retained the ability to interact with CNOT7 after PMA treatment, whereas the ZFP36L1-ΔC mutant did not (Figure 4G). Surprisingly, we also found that PMA treatment still caused an electrophoretic mobility shift of the ZFP36L1-SASA mutant. These results indicate that the interaction between ZFP36L1 and CNOT7 is regulated by ERK-mediated C-terminal phosphorylation of ZFP36L1. Furthermore, C-terminal phosphorylation of ZFP36L1 is not responsible for the PMA-mediated electrophoretic mobility shift.

We considered the possibility that ZFP36 and ZFP36L2 could also be regulated by PMA because the C-terminal region is highly conserved in members of the ZFP36 protein family (Figure 4C). We examined the interaction between CNOT7 and ZFP36 or ZFP36L2 and found that ZFP36L2, in addition to ZFP36 and ZFP36L1, also interacts with CNOT7 and that the interactions between CNOT7 and ZFP36 or ZFP36L2 are inhibited by PMA treatment (Supplementary Figure S5E). Thus, ERK-mediated regulation may be conserved among members of the ZFP36 family.

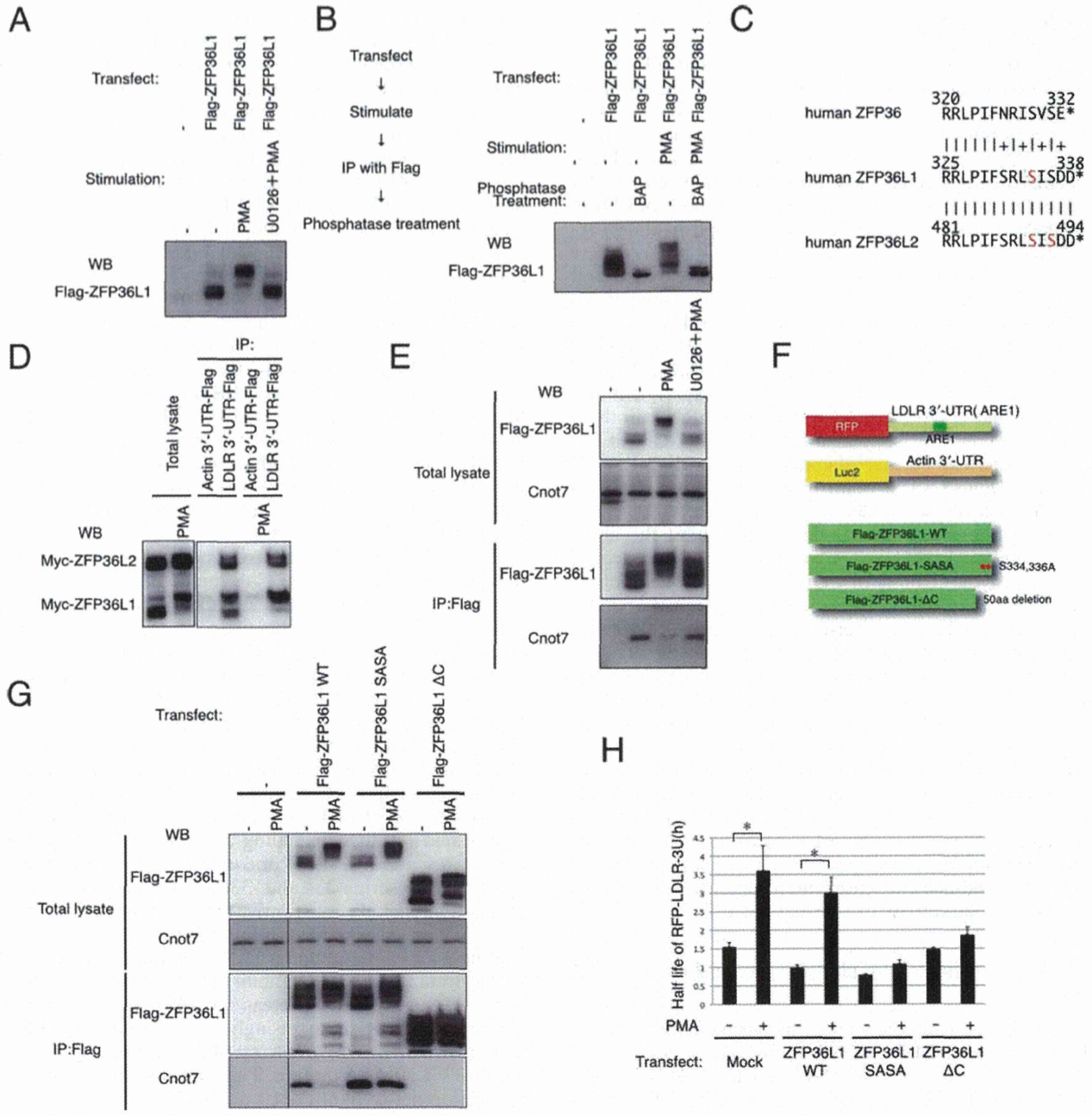

Figure 4. ERK pathway phosphorylates and inhibits ZFP36L2. (**A**) 293T cells were transfected with Flag-tagged ZFP36L1. Twenty-four hours after transfection, cells were treated with PMA (for 30 min) and U0126 (for 45 min), as indicated. Cell lysates were subjected to western blot analysis using anti-Flag antibody. (**B**) 293T cells were transfected with Flag-tagged ZFP36L1. Cells were treated with or without PMA (for 30 min) and the lysates were subjected to IP. Immunopurified Flag-ZFP36L1 was treated with or without bacterial acid phosphatase (BAP) and samples were subjected to western blot analysis using anti-Flag antibody. (**C**) Alignment of C-terminal amino acid sequences in the human ZFP36 family. The C-terminal end of each protein is shown as (*). Identical residues are shown by (l) and similar residues are shown by (+). The serine residues identified as being phosphorylated downstream of ERK are shown in red. (**D**) 293T cells were transfected with Myc-tagged ZFP36L1 or ZFP36L2 and then treated with or without PMA (for 30 min). Cell lysates were subjected to IP using the Flag-antibody and the indicated bait RNAs. Co-immunoprecipitated proteins were subjected to western blot analysis using anti-MYC (9E10) antibody. (**E**) 293T cells were transfected with Flag-tagged ZFP36L1, then treated with PMA (for 30 min) and U0126 (for 45 min) as indicated, and lysates were subjected to IP. Co-immunoprecipitated proteins were subjected to western blot analysis using the indicated antibodies. (**F**) Schematic representation of the constructs used in this experiment. (**G**) 293T cells were transfected with the indicated constructs. Twenty-four hours after transfection, cells were treated with or without PMA (for 30 min), and lysates were subjected to IP. Co-immunoprecipitated proteins were subjected to western blot analysis using the indicated antibodies. (**H**) HeLa cells were transfected with RFP-LDLR 3′-UTR (ARE1) or Luc2-β-Actin-UTR along with the indicated ZFP36L1 constructs. Twenty-four hours after transfection, cells were treated with ActD and PMA (PMA treatment commenced 15 min after ActD treatment), as indicated. Two hours after ActD treatment, cells were harvested and total RNA was extracted. Quantitative RT-PCR (qPCR) was performed using RFP and Luc2-specific primers. Results were normalized to the levels of Luc2 mRNA. The data are representative of at least three independent experiments.

We further validated the function of ZFP36L1 phosphorylation in LDLR mRNA-destabilization. We transfected the RFP-LDLR-3′-UTR expression vector and a luciferase-β-actin-3′-UTR vector along with ZFP36L1-WT, ZFP36L1-SASA or ZFP36L1-ΔC into 293T cells and preformed ActD chase experiments with or without PMA treatment. We observed PMA-mediated stabilization of RFP-LDLR-3′-UTR in mock- and wild-type-ZFP36L1-transfected cells, but not in ZFP36L1-SASA or ZFP36L1-ΔC mutant-transfected cells (Figure 4F and H). These results indicate that ZFP36L1 is regulated by PMA, and that C-terminal phosphorylation of ZFP36L1 is indispensable for ERK-mediated LDLR-mRNA stabilization.

RSK directly phosphorylates ZFP36L1 downstream of ERK

We showed that the C-terminal serine-334 of ZFP36L1 and the C-terminal serine-493 and -495 of ZFP36L2 are phosphorylated downstream of ERK. However, these sites do not match the consensus MAP kinase recognition motifs (SP or TP), indicating that ERK does not directly phosphorylate ZFP36L1. We then examined the possibility that RSK, a major downstream kinase of ERK, directly phosphorylates the C-terminus of ZFP36L1. We first investigated whether BI-D1870 and SL0101, established RSK inhibitors, can reverse PMA-mediated dissociation between ZFP36L1 and CNOT7 protein. We found that BI-D1870 and SL0101 clearly reversed the effect of PMA (Figure 5A, Supplementary Figure S6A). We then examined whether RSK1 directly phosphorylates the C-terminus of ZFP36L1 using recombinant proteins. We incubated *E. coli*-expressed GST-ZFP36L1 with or without active recombinant RSK1 protein under phosphorylation conditions, and analyzed the C-terminal phosphorylation of GST-ZFP36L1 by MS. We found that the C-terminal serine-334 of ZFP36L1 is phosphorylated only when we incubated GST-ZFP36L1 with active RSK1 (Figure 5B and C, Supplementary Figure S6B). We also examined whether active RSK1 inhibits the ability of ZFP36L1 to interact with CNOT proteins. We incubated GST-ZFP36L1 protein with mock buffer, active recombinant ERK1 and/or active recombinant RSK1 under phosphorylation conditions, washed out residual kinase, added 293T cell lysate and performed pulldowns with glutathione-sepharose. We found that GST-ZFP36L1 looses its ability to interact with CNOT1 and CNOT7 proteins when incubated with active recombinant RSK1 (Figure 5D). These results indicate that RSK1 directly phosphorylates the C-terminus of ZFP36L1 downstream of ERK, and inhibits the mRNA destabilization activity of ZFP36L1.

To further confirm our finding that ZFP36L1 and ZFP36L2 are inhibited by PMA treatment, we examined the effect of PMA on the stability of polo-like kinase 3 (PLK3), VEGFA and cellular myelocytomatosis oncogene (cMYC) mRNAs. PLK3 and VEGFA mRNAs have recently been identified as targets of ZFP36L1 (7,8), whereas cMYC mRNA does not bind to ZFP36L1 or ZFP36L2. We found that PLK3 and VEGFA mRNAs were also stabilized by PMA, but that this was not the case for cMYC mRNA (Supplementary Figure S7). These data strongly support the regulation of ZFP36 family proteins by PMA.

DISCUSSION

We have identified ZFP36L1 and ZFP36L2 as two proteins that specifically interact with LDLR mRNA. We showed that ZFP36L1 and ZFP36L2 destabilize LDLR mRNA and that this activity is inhibited by ERK/RSK1 signaling. Recently, KHSRP, hnRNPD and PTBP1 have been reported to be LDLR-destabilizing proteins (5). However, using our approach, we identified KHSRP as a binding protein for the 3′-UTRs of IFNA1, β-actin and cMYC mRNAs and hnRNPD and PTBP1 were common to all the RNA baits. In spite of the binding of these proteins, IFNA1 and β-actin mRNAs were stable, whereas cMYC mRNA was unstable and was not stabilized by ERK signaling. How these proteins selectively regulate the stability of LDLR mRNA is unclear. It is possible that ZFP36L1 and ZFP36L2 coordinately regulate the stability of LDLR mRNA along with KHSRP, hnRNPD and PTBP1.

Target prediction of ZFP36L1 and ZFP36L2

ZFP36L1 and ZFP36L2 belong to the family of CCCH tandem zinc finger proteins (the ZFP36 family), members of which interact with AREs containing a UAUU-UAUU sequence and trigger the degradation of several ARE-containing mRNAs, including PLK3 and VEGFA (7,8,18,19). Consistent with previous reports, we found that ZFP36L1 and ZFP36L2 predominantly interact with the UAUUUAUU sequence of the ARE1 region of the LDLR mRNA, even though the ARE2 region of the LDLR mRNA also contains the same sequence. Interestingly, IFNA1 mRNA, which also has a UAUUUAUU sequence in its 3′-UTR, is stable in cells and ZFP36L1 does not interact strongly with the 3′-UTR of this mRNA (Figure 1B, Supplementary Table S2). Our results suggest that the UAUUUAUU sequence is necessary but not sufficient for ZFP36L1 and ZFP36L2 to interact with and destabilize mRNA. Further investigation is required to predict the target mRNAs of ZFP36L1 and ZFP36L2 *in silico*.

Methods used to identify the regulator of RNA stability

The methods used for (RBP) purification are generally classified into *in vivo* and *in vitro* categories. The *in vivo* purification approach makes use of antisense oligonucleotides, aptamers or MS2-based purification to identify interactions between RNA and RBPs within cells (13,20–24). Use of these methods has elucidated important information on interactions (22–24). On the other hand, the *in vitro* purification approach makes use of cell lysates to purify and identify proteins interacting with *in vitro* synthesized RNA. It is known that some critical regulators of specific RNAs interact specifically with RNA *in vitro* (25). The *in vitro* purification method has several advantages. First, since experimental mRNA expression in cells is not required, this method is sufficiently flexible to enable a wide variety of cells to be used without concerns for transfection efficiency or mRNA expression levels. Second, the amount of bait RNA to be used can be precisely determined to obtain reproducible results that can be subjected to comparison analysis. Third, it is possible to use the RNA sequence of interest, which reduces the amount of nonspecific protein interactions, e.g.

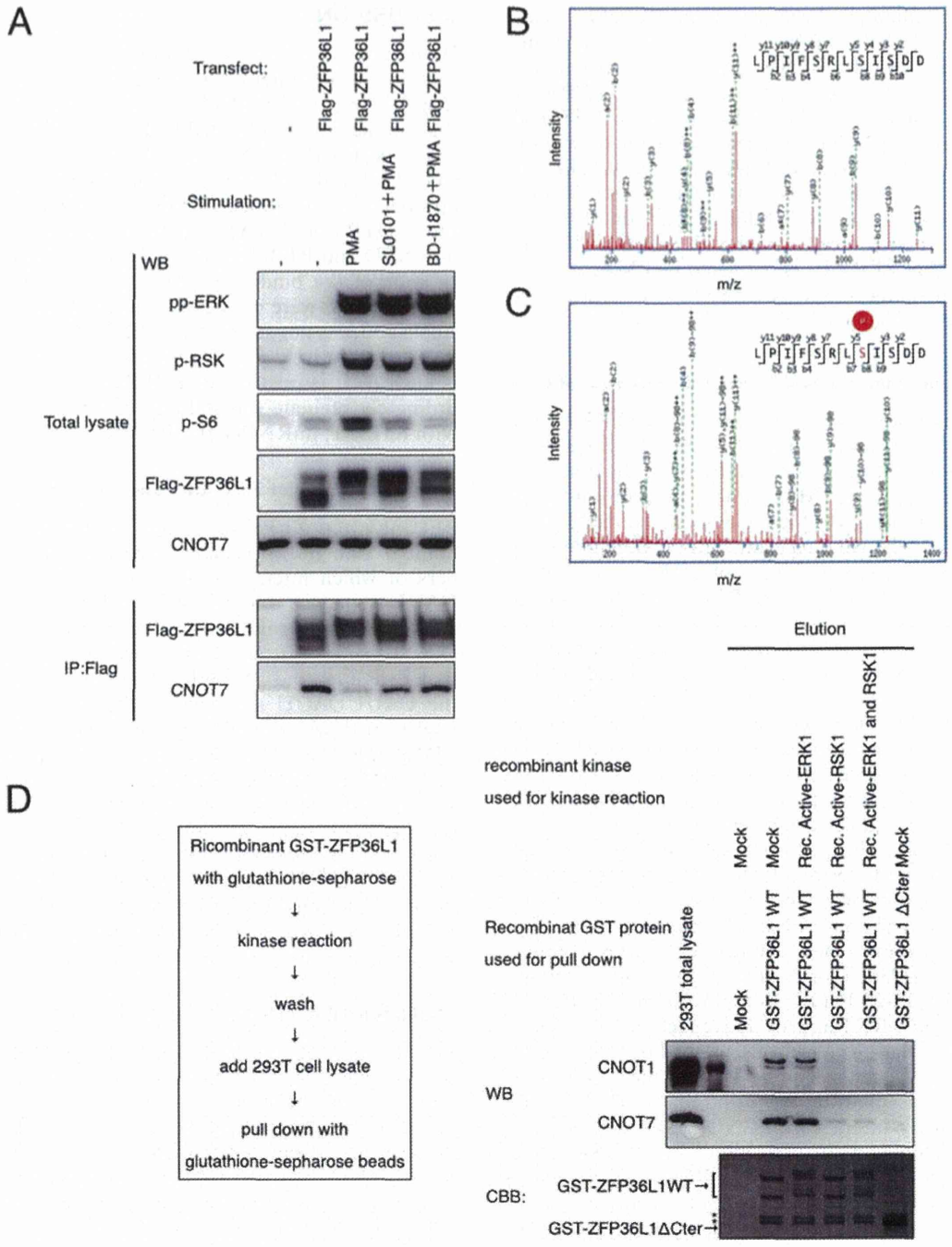

Figure 5. RSK1 directly phosphorylates the C-terminus of ZFP36L1. (**A**) 293T cells were transfected with Flag-tagged ZFP36L1. Twenty-four hours after transfection, cells were treated with PMA (for 30 min) and BI-D1870 or SL0101 (for 45 min) as indicated, and lysates were subjected to IP with the anti-Flag antibody. Co-immunoprecipitated proteins were subjected to western blot analysis using the indicated antibodies. Five percent of the initial amount of cleared 293T lysate was loaded as total lysate. (**B**) GST-ZFP36L1 protein was incubated with or without active recombinant RSK1 under phosphorylation conditions for 30 min. Phosphorylation of GST-ZFP36L1 C-terminal peptide was analyzed by MS. The MS/MS spectrum used to identify the m/z 681.8604-peak as the LPIFSRLSISDD peptide fragment of ZFP36L1 is shown. (**C**) MS/MS spectrum used to identify the m/z 721.8421-peak as the serine-8 phosphorylated LPIFSRLSISDD peptide fragment of ZFP36L1. (**D**) GST-ZFP36L1 protein was incubated with the indicated recombinant kinase under phosphorylation conditions for 30 min, washed, then added to 293T cell lysate and then subjected to pulldown with glutathione-sepharose. Eluted proteins were subjected to western blot analysis using the indicated antibodies and subjected to Coomassie Brilliant Blue (CBB) staining. The asterisk shows a nonspecific band. Five percent of the initial amount of cleared 293T cell lysate was loaded as total lysate. These data are representative of at least three independent experiments.

with ribosomal proteins or PABPs. Given these advantages, plus our fully automated robotic IP and protein identification system, which is highly sensitive and reproducible (11), we opted to use the *in vitro* purification approach, combined with comparison analysis. This allowed us to demonstrate that ZFP36L1 and ZFP36L2 specifically interact with LDLR mRNA, leading to its destabilization. We also identified several known interactions with other bait RNAs including 7SK-CDK9 and 7SK-LARP7. Thus, our results demonstrate that our *in vitro* purification approach is useful for identifying critical regulators of RNAs, which may be used in the identification of important regulators of other types of RNA.

Oligonucleotide-based functional validation

We used RNAi-based knockdown to assess the function of ZRP36L1 and ZFP36L2, but as with many RNA-regulating proteins, ZFP36L1 and ZFP36L2 regulate multiple target mRNAs (6). This makes it difficult to determine whether the result of knockdown is directly caused by inhibition of the interaction between the mRNA and the putative regulator, or is a secondary effect. We therefore performed targeted disruption of the interaction between LDLR-mRNA and ZFP36L1 and ZFP36L2 proteins, using LNA- (9) modified antisense oligonucleotides. LNA is a new-generation artificial nucleotide involving a 2′- and 4′-linked ribose moiety. LNA oligonucleotides have several useful characteristics (26): (i) LNA oligonucleotides are resistant to exo- and endonucleases; (ii) LNA oligonucleotides do not evoke RNase H activity when paired with a complementary RNA strand; (iii) LNA oligonucleotides have very high specificity for complementary RNA and can discriminate even a single-base difference; therefore, short oligonucleotides can be used. Thus, we used LNA-modified antisense oligonucleotides to disrupt the interaction between LDLR and ZFP36L1 and ZFP36L2.

A crucial factor in using antisense-oligonucleotides for such a purpose is to show that the effect of the antisense-oligonucleotide is caused by the interaction between the antisense-oligonucleotide and the intended target mRNA. We have shown several lines of evidence to confirm that the effect of the antisense-oligonucleotide (Oligo-L1) was caused by disrupting the interaction between LDLR mRNA and ZFP36L1 and ZFP36L2: (i) Oligo-L1 could inhibit the interaction between ZFP36L1 and LRLD mRNA, without affecting the interaction between LDLR and hnRNPD, hnRNPI or KHSRP, or the interaction of ZFP36L1 with the 3′-UTRs of PLK3 or VEGFA mRNAs (Supplementary Figure S2B). (ii) Oligo-L1 could stabilize LDLR mRNA in cells (Figure 3F, Supplementary Figure S3G, H and K). (iii) Oligo-L1 could increase the level of LDLR mRNA in cells (Figure 3D). (iv) Oligo-L1 could increase the level of LDLR protein in cells (Figure 3E and G, Supplementary Figure S3E and L). (v) Four control oligonucleotides, Oligo-L2, -L3, -L4, -L5 and -L6, could not inhibit the interaction between LDLR mRNA and ZFP36L1, and also could not increase the levels of LDLR mRNA or protein in cells (Figure 3D, E and G, Supplementary Figure S3E, J and L). These results indicate that the effect of Oligo-L1 is caused by disruption of the interaction between LDLR mRNA and ZFP36L1 and ZFP36L2. These results indicate that LNA-modified antisense oligonucleotides are a powerful tool for validating the function of RBPs. As Cibois *et al.* have also reported (27), antisense oligonucleotides allow us to elucidate the binding sites and the function of RNA/RBP interactions in cells.

In addition to validating the function of the interaction, we were able to increase the amount of LDLR protein in cells. In the liver, the LDLR binds to LDL, thereby lowering blood LDL levels. It has been reported that increasing the amount of LDLR protein in the liver could be a therapeutic approach for hyperlipidemia (28). Recently, some reports have shown that an anti-microRNA antisense oligonucleotide efficiently blocked the function of the microRNA, thereby alleviating diseases in rodents and nonhuman primates (29,30). These results demonstrate the potency of antisense oligonucleotide-based therapeutics. If appropriate delivery of Oligo-L1 to the liver could be achieved, this could result in a candidate drug for the treatment of hyperlipidemia. We believe that Oligo-L1 can be further developed to treat hyperlipidemia. However, it is also very important to consider off-target effects of antisense oligonucleotides, especially with regard to therapeutic applications.

Regulation of ZFP36L1

The CCR4-NOT poly (A) deadenylase complex is composed of more than 10 proteins, including CNOT7. It is known to interact with ZFP36 and ZFP36L1 and to act as an important effector complex of ZFP36-mediated mRNA-destabilization (16,17). We show in this report that PMA treatment causes dissociation of ZFP36L1 and CNOT7, and does not cause the dissociation of LDLR and ZFP36L1/L2 (Figure 4D). In the case of ZFP36L1, the interaction is somewhat increased by PMA treatment (Figure 4D, Supplementary Figure S5B); however, the mechanisms and meaning of enhanced PMA-mediated binding of ZFP36L1 to LDLR mRNA are still unknown. Recently, MAPKAPK2, a downstream kinase of p38, has been shown to phosphorylate ZFP36, but not in the C-terminal region, leading to dissociation of ZFP36 and CNOT7 (16,17). These findings indicate that ZFP36 family proteins are regulated by at least two independent signaling pathways. It is an open question, whether these pathways commonly regulate all ZFP36 family proteins or whether there are differences in regulation between ZFP36 family proteins. It will be important to investigate in detail the mechanisms of these regulatory pathways and to clarify their functional consequences.

SUPPLEMENTARY DATA

Supplementary Data are available at NAR Online.

ACKNOWLEDGMENTS

We thank Y Kawamura, N Goshima, K Shinya, S Chijiwa and T Tuchiura for providing reagents. We thank K Nakamura for excellent technical assistance. We also thank M Oubihi, T Hirose and K Horimoto for helpful discussions.

FUNDING

Galaxy Pharma Inc. Funding for open access charge: National Institute of Advanced Industrial Science and Technology.

Conflict of interest statement. None declared.

REFERENCES

1. Bakheet,T., Williams,B.R. and Khabar,K.S. (2006) ARED 3.0: the large and diverse AU-rich transcriptome. *Nucleic Acids Res.*, **34**, 111–114.
2. Barreau,C., Paillard,L. and Osborne,H.B. (2006) AU-rich elements and associated factors: are there unifying principles? *Nucleic Acids Res.*, **33**, 7138–7150.
3. Goa,G-W. and Mania,A. (2012) Low-density lipoprotein receptor (LDLR) family orchestrates cholesterol homeostasis. *Yale J. Biol. Med.*, **85**, 19–28.
4. Kong,W., Wei,J., Abidi,P., Lin,M., Inaba,S., Li,C., Wang,Y., Wang,Z., Si,S., Pan,H. *et al.* (2004) Berberine is a novel cholesterol-lowering drug working through a unique mechanism distinct from statins. *Nat. Med.*, **10**, 1344–1351.
5. Li,H., Chen,W., Zhou,Y., Abidi,P., Sharpe,O., Robinson,W.H., Kraemer,F.B. and Liu,J. (2009) Identification of mRNA binding proteins that regulate the stability of LDL receptor mRNA through AU-rich elements. *J. Lipid. Res.*, **50**, 820–831.
6. Sanduja,S., Blanco,F.F. and Dixon,D.A. (2011) The roles of TTP and BRF proteins in regulated mRNA decay. *Wiley Interdiscip. Rev. RNA*, **1**, 42–57.
7. Horner,T.J., Lai,W.S., Stumpo,D.J. and Blackshear,P.J. (2009) Stimulation of polo-like kinase 3 mRNA decay by tristetraprolin. *Mol. Cell. Biol.*, **29**, 1999–2010.
8. Hacker,C., Valchanova,R., Adams,S. and Munz,B. (2010) ZFP36L1 is regulated by growth factors and cytokines in keratinocytes and influences their VEGF production. *Growth Factors*, **28**, 178–190.
9. Kauppinen,S., Vester,B. and Wenge,J. (2005) Locked nucleic acid (LNA): high affinity targeting of RNA for diagnostics and therapeutics. *Drug Discov. Today*, **2**, 287–290.
10. Kourouklis,D., Murakami,H. and Suga,H. (2005) Programmable ribozymes for mischarging tRNA with nonnatural amino acids and their applications to translation. *Methods*, **36**, 239–244.
11. Iemura,S.I. and Natsume,T. (2012) One-by-one sample preparation method for protein network analysis. In Cai,J. (ed). *Protein Interaction*. Intech, Rijeka, Croatia, pp. 293–310.
12. Matsumoto,M., Oyamada,K., Takahashi,H., Sato,T., Hatakeyama,S. and Nakayama,K.I. (2009) Large-scale proteomic analysis of tyrosine- phosphorylation induced by T-cell receptor or B-cell receptor activation reveals new signaling pathways. *Proteomics*, **9**, 3549–3563.
13. Said,N., Rieder,R., Hurwitz,R., Deckert,J., Urlaub,H. and Vogel,J. (2009) In vivo expression and purification of aptamer-tagged small RNA regulators. *Nucleic Acids Res.*, **37**, e133.
14. Diribarne,G. and Bensaude,O. (2009) 7SK RNA, a non-coding RNA regulating P-TEFb, a general transcription factor. *RNA Biol.*, **6**, 122–128.
15. Seonmi,S., Yea,S.K., Jisu,K., Hyun-Mi,K., Dong-Eun,K. and Sang,S.H. (2013) Sniffing for gene-silencing efficiency of siRNAs in HeLa cells in comparison with that in HEK293T cells: correlation between knockdown efficiency and sustainability of siRNAs revealed by FRET-based probing. *Nucleic Acid Ther.*, **23**, 152–159.
16. Marchese,F.P., Aubareda,A., Tudor,C., Saklatvala,J., Clark,A.R. and Dean,J.L. (2010) MAPKAP kinase 2 blocks tristetraprolin-directed mRNA decay by inhibiting CAF1 deadenylase recruitment. *J. Biol. Chem.*, **285**, 27590–27600.
17. Sandler,H., Kreth,J., Timmers,H.T. and Stoecklin,G. (2011) Not1 mediates recruitment of the deadenylase Caf1 to mRNAs targeted for degradation by tristetraprolin. *Nucleic Acids Res.*, **10**, 4373–4386.
18. Hudson,B.P., Martinez-Yamout,M.A., Dyson,H.J. and Wright,P.E. (2004) Recognition of the mRNA AU-rich element by the zinc finger domain of TIS11d. *Nat. Struct. Mol. Biol.*, **11**, 257–264.
19. Duan,H., Cherradi,N., Feige,J.J. and Jefcoate,C. (2009) cAMP-dependent posttranscriptional regulation of steroidogenic acute regulatory (STAR) protein by the zinc finger protein ZFP36L1/TIS11b. *Mol. Endocrinol.*, **23**, 497–509.
20. Wassarman,D.A. and Steitz,J.A. (1991) Structural analyses of the 7SK ribonucleoprotein (RNP), the most abundant human small RNP of unknown function. *Mol. Cell. Biol.*, **11**, 3432–3445.
21. Yang,Z., Zhu,Q., Luo,K. and Zhou,Q. (2001) The 7SK small nuclear RNA inhibits the CDK9/cyclin T1 kinase to control transcription. *Nature*, **414**, 317–322.
22. Vasudevan,S. and Steitz,J.A. (2007) AU-rich-element-mediated upregulation of translation by FXR1 and Argonaute 2. *Cell*, **128**, 1105–1118.
23. Hogg,J.R. and Collins,K. (2007) RNA-based affinity purification reveals 7SK RNPs with distinct composition and regulation. *RNA*, **13**, 868–880.
24. Bessonov,S., Anokhina,M., Will,C.L., Urlaub,H. and Lührmann,R. (2008) Isolation of an active step I spliceosome and composition of its RNP core. *Nature*, **452**, 846–850.
25. Townley-Tilson,W.H., Pendergrass,S.A., Marzluff,W.F. and Whitfield,M.L. (2006) Genome-wide analysis of mRNAs bound to the histone stem-loop binding protein. *RNA*, **12**, 1853–1867.
26. Obika,S., Nanbu,D., Hari,Y., Andoh,J., Morio,K., Doi,T. and Imanishi,T. (1998) Stability and structural features of the duplexes containing nucleoside analogues with a fixed N-type conformation, 2′-O,4′-C-methyleneribonucleosides. *Tetrahedron Lett.*, **39**, 5401–5404.
27. Cibois,M., Gautier-Courteille,C., Vallée,A. and Paillard,L. (2010) A strategy to analyze the phenotypic consequences of inhibiting the association of an RNA-binding protein with a specific RNA. *RNA*, **16**, 10–15.
28. Garg,A. and Simha,V. (2007) Update on dyslipidemia. *J. Clin. Endocrinol. Metab.*, **92**, 1581–1589.
29. Elmén,J., Lindow,M., Schütz,S., Lawrence,M., Petri,A., Obad,S., Lindholm,M., Hedtjärn,M., Hansen,H.F., Berger,U. *et al.* (2008) LNA-mediated microRNA silencing in non-human primates. *Nature*, **452**, 896–899.
30. Lanford,R.E., Hildebrandt-Eriksen,E.S., Petri,A., Persson,R., Lindow,M., Munk,M.E., Kauppinen,S. and Ørum,H. (2010) Therapeutic silencing of microRNA-122 in primates with chronic hepatitis C virus infection. *Science*, **327**, 198–201.

MCB
Journals.ASM.org

MDM2 Mediates Nonproteolytic Polyubiquitylation of the DEAD-Box RNA Helicase DDX24

Takayoshi Yamauchi, Masaaki Nishiyama, Toshiro Moroishi, Kanae Yumimoto, Keiichi I. Nakayama

Department of Molecular and Cellular Biology, Medical Institute of Bioregulation, Kyushu University, Higashi-ku, Fukuoka, Fukuoka, and CREST, Japan Science and Technology Agency (JST), Kawaguchi, Saitama, Japan

MDM2 mediates the ubiquitylation and thereby triggers the proteasomal degradation of the tumor suppressor protein p53. However, genetic evidence suggests that MDM2 contributes to multiple regulatory networks independently of p53 degradation. We have now identified the DEAD-box RNA helicase DDX24 as a nucleolar protein that interacts with MDM2. DDX24 was found to bind to the central region of MDM2, resulting in the polyubiquitylation of DDX24 both *in vitro* and *in vivo*. Unexpectedly, however, the polyubiquitylation of DDX24 did not elicit its proteasomal degradation but rather promoted its association with preribosomal ribonucleoprotein (pre-rRNP) processing complexes that are required for the early steps of pre-rRNA processing. Consistently with these findings, depletion of DDX24 in cells impaired pre-rRNA processing and resulted both in abrogation of MDM2 function and in consequent p53 stabilization. Our results thus suggest an unexpected role of MDM2 in the nonproteolytic ubiquitylation of DDX24, which may contribute to the regulation of pre-rRNA processing.

MDM2 belongs to the family of RING finger-type ubiquitin ligases (E3s) and functions as a pivotal negative regulator of the tumor suppressor protein p53 (1, 2). MDM2 inhibits p53 function by two distinct mechanisms: it abrogates the transactivation activity of p53 through direct binding to the NH_2-terminal region of the protein (3, 4), and it mediates the polyubiquitylation of p53 and thereby targets it for degradation by the 26S proteasome (5–7). On the other hand, p53 binds to the promoter of the MDM2 gene and activates its expression (8, 9), thereby completing a negative-feedback loop that is responsible for strict regulation of p53 function in the absence of stress. Exposure of cells to stress, however, results in downregulation of both the abundance and the activity of MDM2 as well as consequent stabilization and subsequent activation of p53 (1, 2). The mechanisms by which p53 escapes from the inhibitory action of MDM2 differ among cell types and stress signals.

The role of the nucleolus as a stress sensor has recently emerged. Many types of stress signal converge on steps of ribosome biogenesis and thereby activate p53 (10). A group of ribosomal proteins (RPs), including RPL5, RPL11, and RPL23, serve as transmitters of stress signaling. These proteins are released from the nucleolus in response to stress, bind to and inhibit the activity of MDM2 in the nucleoplasm (11), and eventually activate p53 (11–18).

Inhibition of precursor rRNA (pre-rRNA) processing is a key mechanism for induction of nucleolar stress (19). In mammals, the ~200 genes encoding 47S pre-rRNA, which serves as a precursor for 18S, 5.8S, and 28S rRNAs, are organized in five tandem arrays on the short arms of acrocentric chromosomes. These genes are transcribed by RNA polymerase I (Pol I) in association with the Pol I-specific basal factors SL1 (also known as TAF1B) and UBF (20). The transcribed 47S pre-rRNA undergoes a series of endo- and exonucleolytic cleavages to remove the spacer sequences. In addition, the pre-rRNA is subjected to covalent modifications that include base and ribose methylation as well as uridine isomerization to pseudouridine at specific sites (21, 22). During this process, many assembly factors are associated with the pre-rRNA and its processing products in the form of a preribosomal ribonucleoprotein (pre-rRNP) complex (23). Proteomic characterization of human pre-rRNP complexes has identified >180 assembly factors and 100 small nucleolar ribonucleoprotein particles (snoRNPs) involved in this process (24–27).

DEAD-box RNA helicases constitute a group of such assembly factors, although their precise roles in ribosome biogenesis have not been fully characterized. These enzymes participate in the regulation of essentially all aspects of RNA metabolism, including pre-mRNA splicing, translation, pre-rRNA processing, and mRNA decay. Most of them have been highly conserved through evolution, and many have been shown to contribute to ribosome biogenesis in yeasts (28, 29).

With a proteomics approach, we have now identified proteins that are associated with MDM2 in human cells. Among these MDM2 binding proteins, we focused on DDX24, a nucleolar protein that belongs to the family of DEAD-box RNA helicases. Although MAK5, the *Saccharomyces cerevisiae* ortholog of human DDX24, was previously found to contribute to the biosynthesis of the 60S ribosome subunit (30), the function of DDX24 in mammals has remained unclear. We found that DDX24 binds to the central acidic region of MDM2 and that such binding promotes the polyubiquitylation of DDX24. However, the polyubiquitylation of DDX24 did not elicit its proteasomal degradation but rather promoted its association with components of pre-rRNP complexes that are required for efficient pre-rRNA processing reactions. Depletion of DDX24 by RNA interference (RNAi) inhibited proper pre-rRNA processing. Our findings thus demonstrate the existence of MDM2-mediated noncanonical polyubiquitylation in human cells.

Received 7 March 2014 Returned for modification 11 April 2014
Accepted 23 June 2014
Published ahead of print 30 June 2014
Address correspondence to Keiichi I. Nakayama, nakayak1@bioreg.kyushu-u.ac.jp.

doi:10.1128/MCB.00320-14

TABLE 1 Proteins identified by LC-MS/MS analysis of tryptic peptides derived from endogenous proteins captured by FLAG-MDM2 expressed in HCT116 cells

Protein function(s) and name	UniProt accession no.	Yeast ortholog	Domain(s)[a]	No. of peptides
DNA repair				
HMGB1	P09429	NHP6B	HMG box	4
HMGB2	P26583	NHP6B	HMG box	3
XRCC5	P13010	YKU80	Leucine zipper, Ku	2
Protein and RNA metabolism				
RPL11	P62913	RPL11A		10
RPL3	P39023	RPL3		4
RPL9	P32969	RPL9B		3
RPS10	P46783	RPS10A		3
RPS14	P62263	RPS14A		4
RPS19	P39019	RPS19A		3
RPS2	P15880	RPS2	S5 DRBM	6
RPS25	P62851	RPS25A		3
RPS3A	P61247	RPS1A		9
RPS6	P62753	RPS6A		7
RPS7	P62081	RPS7A		8
RPS9	P46781	RPS9A	S4 RNA binding	5
RNA metabolism, splicing, processing				
DDX24	Q9GZR7	MAK5	Helicase	12
WDR77	Q9BQA1	PFS2	WD repeats	14
HNRNPF	P52597		RRM	4
HNRNPH1	P31943		RRM	6
HNRNPK	P61978	PBP2	RGG box, KH	6
RBM10	Q6PKH5		RRM, G patch, zinc finger	18
SNRNP200	O75643	BRR2	Helicase, SEC63, coiled coil	8
GRWD1	Q9BQ67	RRB1	WD repeats	4
NCL	P19338	NSR1	RRM	9
TRMT10C	Q7L0Y3	TRM10	Coiled coil	7
Protein metabolism				
CCT2	P78371	CCT2		10
CCT4	P50991	CCT4		7
CCT5	P48643	CCT5		6
PSMC2	P35998	RPT1		2
TCP1	P17987	TCP1		10
Lipid metabolism: HADHA	P40939	EHD3		30
Signal transduction, phosphorylation, ubiquitylation				
NPM1	P06748			6
TP53	P04637		DNA binding	9
YWHAB	P31946	BMH2		6
YWHAQ	P27348	BMH2		6
CDK9	P50750	CTK1	Protein kinase	4
STK38	Q15208	CBK1	Protein kinase, AGC kinase	14
STK38L	B4E3J8	CBK1	Protein kinase, AGC kinase	8
PIP4K2C	Q8TBX8	MSS4	PIPK	4
TRIM21	P19474		B30.2/SPRY, zinc finger, coiled coil	9
Regulation of transcription: THRAP3	Q9Y2W1			10
Cell adhesion: EZR	P15311		FERM	3

[a] HMG, high mobility group; DRBM, double-stranded RNA binding motif; RRM, RNA recognition motif; KH, K homology; PIPK, phosphatidylinositol phosphatase kinases; FERM, four-point-one, ezrin, radixin, moesin.

MATERIALS AND METHODS

Plasmids. Complementary DNAs encoding wild-type (WT) or mutant forms of human or mouse MDM2 as well as human DDX24, DDX24-ub, p53, p53-ub, ubiquitin, nucleolin (NCL), NIP7, p14ARF, RPL5, RPL11, RPL23, RPL26, and RPS7, each tagged at its NH_2 terminus with FLAG, hemagglutinin (HA), Myc, or green fluorescent protein (GFP) epitopes, were subcloned into pcDNA3 (Invitrogen), pRSET (Invitrogen), or pGEX6p (GE Healthcare). A cDNA encoding human ubiquitin, tagged at